Interstellar, space and planetary plasmas

https://doi.org/10.1017/S1743921311006569 Published online by Cambridge University Press

Advances in Plasma Astrophysics
Proceedings IAU Symposium No. 274, 2010
A. Bonanno, E. de Gouveia Dal Pino & A. G. Kosovichev, eds.
© International Astronomical Union 2011
doi:10.1017/S1743921311006569

A new viscous instability in weakly ionised protoplanetary discs

Anders Johansen[1], Mariko Kato[2] and Takayoshi Sano[3]

[1]Lund Observatory, Lund University
Box 43, 221 00 Lund, Sweden
email: anders@astro.lu.se

[2]Department of Earth and Planetary Science, Tokyo Institute of Technology
Ookayama 2-1-12-I2-10, Meguro-ku, Tokyo, Japan
email: marikok@geo.titech.ac.jp

[3]Institute of Laser Engineering, Osaka University
Suita, Osaka 565-0871, Japan
email: sano@ile.osaka-u.ac.jp

Abstract. Large regions of protoplanetary discs are believed to be too weakly ionised to support magnetorotational instabilities, because abundant tiny dust grains soak up free electrons and reduce the conductivity of the gas. At the outer edge of this "dead zone", the ionisation fraction increases gradually and the resistivity drops until the magnetorotational instability can develop turbulence. We identify a new viscous instability which operates in the semi-turbulent transition region between "dead" and "alive" zones. The strength of the saturated turbulence depends strongly on the local resistivity in this transition region. A slight increase (decrease) in dust density leads to a slight increase (decrease) in resistivity and a slight decrease (increase) in turbulent viscosity. Such spatial variation in the turbulence strength causes a mass pile-up where the turbulence is weak, leading to a run-away process where turbulence is weakened and mass continues to pile up. The final result is the appearance of high-amplitude pressure bumps and deep pressure valleys. Here we present a local linear stability analysis of weakly ionised accretion discs and identify the linear instability responsible for the pressure bumps. A paper in preparation concerns numerical results which confirm and expand the existence of the linear instability.

Keywords. accretion, accretion disks, (magnetohydrodynamics:) MHD, turbulence, (stars:) planetary systems: formation, (stars:) planetary systems: protoplanetary disks

1. Introduction

Consider a protoplanetary disc irradiated with a cosmic ray flux F (particles per area per unit time). The reduction of the flux is controlled by the equation

$$\frac{\mathrm{d}F}{\mathrm{d}z} = -\kappa\rho(z)F(z)\,, \tag{1.1}$$

where κ is the opacity and ρ is the z-dependent mass density. The solution is

$$F_\downarrow(z) = F_\infty \exp[-\kappa\Sigma_\uparrow(z)]\,, \tag{1.2}$$

$$F_\uparrow(z) = F_\infty \exp[-\kappa\Sigma_\downarrow(z)]\,. \tag{1.3}$$

Here $\Sigma_\uparrow(z) = \int_z^\infty \rho(z)\mathrm{d}z$ is the column density of gas above the given point, while $\Sigma_\downarrow(z) = \int_{-\infty}^z \rho(z)\mathrm{d}z$ is the column density below. We have $\Sigma = \Sigma_\uparrow(z) + \Sigma_\downarrow(z)$ at all z. Introducing the ionisation rate $\zeta(z)$ we get (Sano *et al.* 2000)

$$\zeta(z) = \frac{\zeta_{\rm CR}}{2}\left\{\exp[-\Sigma_\uparrow(z)/\Sigma_{\rm CR}] + \exp[-\Sigma_\downarrow(z)/\Sigma_{\rm CR}]\right\}\,. \tag{1.4}$$

https://doi.org/10.1017/S1743921311006569 Published online by Cambridge University Press

Here $\zeta_{\rm CR}$ is the ionisation rate by cosmic rays in interstellar space and $\Sigma_{\rm CR} = 1/\kappa$ is the penetration column density of cosmic rays. Free electrons are lost as they collide with dust grains. This yields the rate equation

$$\frac{\partial n_{\rm e}}{\partial t} = \zeta n_{\rm n} - n_{\rm e} n_\bullet \langle \sigma v \rangle_{{\rm e},\bullet} \tag{1.5}$$

for electron number density $n_{\rm e}$. Here $\zeta = \kappa m_{\rm n} F$ is the ionisation rate. The equilibrium electron density fraction is

$$\frac{n_{\rm e}}{n_{\rm n}} = \frac{\zeta}{n_\bullet \langle \sigma v \rangle_{{\rm e},\bullet}} \,. \tag{1.6}$$

This expression is valid in the limit of negligible gas phase recombination and is equivalent to the *ion-dust plasma* limit of Okuzumi (2009). The resistivity of the electrons is given in c.g.s. units by

$$\eta = \frac{c^2}{4\pi\sigma_{\rm e}} \,, \tag{1.7}$$

where c is the speed of light and $\sigma_{\rm e}$ is the electrical conductivity. In turn the conductivity is given by

$$\sigma_{\rm e} = \frac{n_{\rm e} e^2}{m_{\rm e} \nu} \,. \tag{1.8}$$

Here $n_{\rm e}$ is the number density of electrons, e is the electron charge, $m_{\rm e}$ is the electron mass, and ν is the collision frequency of electrons with neutrals. The momentum rate coefficient $\langle \sigma v \rangle = \nu / n_{\rm n}$ for transfer of momentum from electrons to neutrals is given by $\langle \sigma v \rangle = 8.3 \times 10^{-10} T^{1/2}\,{\rm cm^3\,s^{-1}}$. This finally yields (Blaes & Balbus 1994)

$$\eta = 230 \left(\frac{n_{\rm n}}{n_{\rm e}} \right) T^{1/2}\,{\rm cm^2\,s^{-1}} \,. \tag{1.9}$$

Together with equation (1.6) and equation (1.4) this gives us a model for the resistivity in protoplanetary discs, provided that we know $\zeta_{\rm CR}$ of the cosmic rays, $\rho(z)$ and $\Sigma_{\rm CR}$ for the gas, and number density $n_{\rm d}$ and collision cross section $\sigma_{\rm d}$ of the dust grains.

The fastest growing wavenumber for the MRI is

$$k_{\rm BH} = \sqrt{\frac{15}{16}} \frac{v_{\rm A}}{\Omega} \,, \tag{1.10}$$

where $v_{\rm A} = B_0 / \sqrt{\mu_0 \rho}$ is the vertical Alfvén speed and B_0 is the constant vertical magnetic field component. The MRI can grow when the Elsasser number $\Lambda_{\rm MRI}$ fulfills

$$\Lambda_{\rm MRI} = \frac{v_{\rm A}^2}{\eta \Omega} \gtrsim 1 \,. \tag{1.11}$$

For the Minimum Mass Solar Nebula the Elsasser number in the mid-plane scales with r^{-4}, assuming that $\Sigma \ll \Sigma_{\rm CR}$ and constant $\beta = P_{\rm gas}/P_{\rm mag}$.

We set the rate coefficients for collisions between electrons and dust grains as

$$\langle \sigma v \rangle_{{\rm e},\bullet} = \pi a_\bullet^2 c_{\rm e} \,, \tag{1.12}$$

where $c_{\rm e}$ is the thermal speed of the electrons.

$$c_{\rm e} = \sqrt{\frac{8 k_{\rm B} T}{\pi m_{\rm e}}} \,. \tag{1.13}$$

This simple approach allows us to calculate the resistivity of the gas anywhere in the disc at a relatively modest computational cost.

https://doi.org/10.1017/S1743921311006569 Published online by Cambridge University Press

2. Stability analysis

We proceed now to analyse the stability of a turbulent accretion disc with turbulent stress S and turbulent diffusion D_t. We work in the shearing sheet formalism, representing a small corotating box at an arbitrary distance from the central star. The constant Keplerian angular frequency is Ω. The gas velocity relative to the main Keplerian flow is $\boldsymbol{u}$ and the velocity of the dust component is $\boldsymbol{w}$. The gas density and the dust number are denoted ρ_g and n_d. We consider an isothermal equation of state with constant sound speed c_s. Dust is coupled to the gas via a drag force working on the time-scale τ_f. The dynamical equations are

$$\frac{\mathrm{D}u_x}{\mathrm{D}t} = 2\Omega u_y - \frac{c_\mathrm{s}^2}{\rho_\mathrm{g}}\frac{\partial \rho_\mathrm{g}}{\partial x}\,, \tag{2.1}$$

$$\frac{\mathrm{D}u_y}{\mathrm{D}t} = -\frac{1}{2}\Omega u_x - \frac{1}{\rho_\mathrm{g}}\frac{\partial S}{\partial x}\,, \tag{2.2}$$

$$\frac{\mathrm{D}\rho_\mathrm{g}}{\mathrm{D}t} = -\rho_\mathrm{g}\frac{\partial u_x}{\partial x} + D_\mathrm{t}\frac{\partial^2 \rho_\mathrm{g}}{\partial x^2}\,, \tag{2.3}$$

$$\frac{\mathrm{D}w_x}{\mathrm{D}t} = 2\Omega w_y - \frac{1}{\tau_\mathrm{f}}(w_x - u_x)\,, \tag{2.4}$$

$$\frac{\mathrm{D}w_y}{\mathrm{D}t} = -\frac{1}{2}\Omega w_x - \frac{1}{\tau_\mathrm{f}}(w_y - u_y)\,, \tag{2.5}$$

$$\frac{\mathrm{D}n_\mathrm{d}}{\mathrm{D}t} = -n_\mathrm{d}\frac{\partial w_x}{\partial x} + D_\mathrm{t}\frac{\partial^2 n_\mathrm{d}}{\partial x^2}\,. \tag{2.6}$$

Here $\mathrm{D}/\mathrm{D}t \equiv \partial/\partial t + (\boldsymbol{u}\cdot\boldsymbol{\nabla}) - (3/2)\Omega x\partial/\partial y$. Going in the limit of short friction times we get the simplification

$$w_x = u_x + \tau_\mathrm{f}\frac{c_\mathrm{s}^2}{\rho_\mathrm{g}}\frac{\partial \rho_\mathrm{g}}{\partial x}\,, \tag{2.7}$$

$$w_y = u_y + \tau_\mathrm{f}\frac{1}{\rho_\mathrm{g}}\frac{\partial S}{\partial x}\,. \tag{2.8}$$

The viscous instability arises from the dependence of S on n_d. We linearise the equation system around the state with gas density ρ_0 and dust number density n_0 and define the particle-stress coupling parameter of the background state $\chi = \partial \ln S/\partial \ln n_\mathrm{d}$. When the Elsasser number is smaller than unity we expect that $\chi \sim 1$ (Pessah 2010). We ignore turbulent diffusion D_t in the linearisation. We consider axisymmetric perturbations with $f(x,t) = \hat{f}\exp[\mathrm{i}(k_x x - \omega t)]$.

The resulting linearised equation system can be put on the matrix form $\boldsymbol{M}\hat{\boldsymbol{f}} = 0$, where $\hat{\boldsymbol{f}} = (\hat{u}_x, \hat{u}_y, \hat{\rho}_\mathrm{g}, \hat{n}_\mathrm{d})$ is a vector of complex amplitudes and $\boldsymbol{M}$ is

$$\begin{pmatrix} \mathrm{i}\omega & 2\Omega & -c_\mathrm{s}^2/\rho_0\mathrm{i}k_x & 0 \\ -(1/2)\Omega & \mathrm{i}\omega & 0 & (\chi/n_0)(S_0/\rho_0)\mathrm{i}k_x \\ -\rho_0\mathrm{i}k_x & 0 & \mathrm{i}\omega & 0 \\ -n_0\mathrm{i}k_x & 0 & (n_0/\rho_0)\tau_\mathrm{f}c_\mathrm{s}^2k_x^2 & \mathrm{i}\omega\,. \end{pmatrix} \tag{2.9}$$

We have only non-trivial solutions when the determinant of the matrix is zero. The dispersion relation is

$$0 = \omega^2(\omega^2 - c_\mathrm{s}^2k_x^2 - \Omega^2) - \frac{2k_x^2\Omega S_0\chi}{\rho_0}(c_\mathrm{s}^2k_x^2\tau_\mathrm{f} - \mathrm{i}\omega)\,. \tag{2.10}$$

This equation can be solved numerically to find four complex frequencies for each

https://doi.org/10.1017/S1743921311006569 Published online by Cambridge University Press

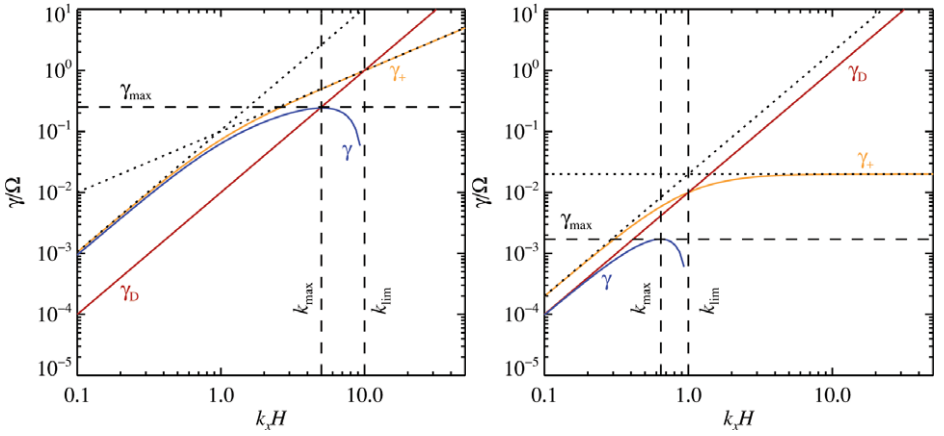

Figure 1. The growth rate γ_+ as a function of radial wavenumber k_x, based on a numerical solution to equation (2.10). Left plot: parameters are $\Omega = c_\mathrm{s} = \rho_0 = \tau_\mathrm{f} = 1$ and $S_0 = 0.01$. The maximum growth rate, $\gamma_{\mathrm{max}} = 0.25\Omega$, occurs at $k_{\mathrm{max}} = 5H^{-1}$, while the highest wavenumber for growth is $k_{\mathrm{lim}} = 10H^{-1}$. The two solution branches, following the limiting solutions found in equations (2.15) and (2.14), are indicated with dotted lines. Right plot: same as left plot but with passive particles ($\tau_\mathrm{f} = 0$). The instability for passive particles occurs at longer wavelengths and at lower growth rates.

wavenumber. However, a simplification of the equation system allows us to find two analytical solutions instead.

Assuming geostrophic balance $0 = 2\Omega u_y - c_\mathrm{s}^2(\partial \ln \rho_\mathrm{g}/\partial x)$ instead of equation (2.1), the dispersion relation simplifies to the second order expression

$$0 = \omega^2(-c_\mathrm{s}^2 k_x^2 - \Omega^2) - \frac{2k_x^2 \Omega S_0 \chi}{\rho_0}(c_\mathrm{s}^2 k_x^2 \tau_\mathrm{f} - \mathrm{i}\omega)\,. \tag{2.11}$$

The approximation that geostrophic balance is always maintained effectively filters away high frequency density waves that are of no importance for the viscous drift instability. The two solutions to equation (2.11) are

$$\omega_\pm = \frac{1}{1 + k_x^2 H^2} k_x^2 \frac{S_0 \chi}{\Omega \rho_0} \left[1 \pm \sqrt{1 + (1 + k_x^2 H^2)\,\frac{2c_\mathrm{s}^2 \Omega \tau_\mathrm{f} \rho_0}{S_0 \chi}}\right] \mathrm{i}\,. \tag{2.12}$$

One solution is complex positive (instability), while the other is always complex negative (damped mode). In the two limits of $k_x H$ the growth rate $\gamma_+ = \mathrm{Im}(\omega_+)$ of the positive solution is

$$k_x H \gg 1 : \gamma_+ = \frac{1}{H^2} \frac{S_0 \chi}{\Omega \rho_0} \left(1 + \sqrt{1 + k_x^2 H^2 \frac{2c_\mathrm{s}^2 \Omega \tau_\mathrm{f} \rho_0}{S_0 \chi}}\right), \tag{2.13}$$

$$k_x H \ll 1 : \gamma_+ = k_x^2 \frac{S_0 \chi}{\Omega \rho_0} \left(1 + \sqrt{1 + \frac{2c_\mathrm{s}^2 \Omega \tau_\mathrm{f} \rho_0}{S_0 \chi}}\right). \tag{2.14}$$

The high wavenumber branch can further be expanded as

$$k_x H \gg \sqrt{S_0 \chi/(2c_\mathrm{s}^2 \Omega \tau_\mathrm{f} \rho_0)} : \ \gamma_+ = k_x \sqrt{\frac{2\Omega \tau_\mathrm{f} S_0 \chi}{\rho_0}}\,. \tag{2.15}$$

This limit is only relevant if $S_0 \chi/(2c_\mathrm{s}^2 \Omega \tau_\mathrm{f} \rho_0) > 1$.

https://doi.org/10.1017/S1743921311006569 Published online by Cambridge University Press

The growth rate of the viscous drift instability tends towards infinity for infinitely high wave numbers, according to equation (2.15). The linear scaling with k_x, however, implies that turbulent diffusion will stabilise the mode at high wavenumbers. Turbulent diffusion of the particles has a damping rate of

$$\gamma_{\rm D} = -k_x^2 D_{\rm t} = -k_x^2 \frac{S_0}{\Omega \rho_0}\,. \tag{2.16}$$

The limiting wavenumber for instability, where $\gamma = \gamma_{\rm D} + \gamma_+ = 0$, is

$$k_{\rm lim}^2 H^2 = 2\chi \left(1 + \frac{c_{\rm s}^2 \Omega \tau_{\rm f} \rho_0}{S_0}\right) - 1\,. \tag{2.17}$$

The most unstable wavenumber has no simple analytical form in the general case. However, in the case of mobile dust particles with $\Omega_{\rm f}\tau_{\rm f} > 0$ we find the most unstable wavenumber in the high wavenumber branch, because of the different wavenumber scaling of instability and turbulent damping. The most unstable wavenumber is

$$k_{\rm max} = \sqrt{\frac{\Omega^3 \tau_{\rm f} \chi \rho_0}{2 S_0}}\,, \tag{2.18}$$

which is two times the limiting wavenumber. Weaker (stronger) turbulence has maximum growth rate at shorter (longer) wavelengths. For typical parameters we find a wavelength for maximum growth around a few scale heights in the radial direction. The highest growth rate is

$$\gamma_{\rm max}/\Omega = \frac{1}{2}\chi \Omega \tau_{\rm f}\,, \tag{2.19}$$

which shows clearly the importance of freedom in the motion of the particles relative to the gas. The dependence of the growth rate on the wavenumber is shown in Figure 1 for typical values relevant to a protoplanetary disc.

2.1. *Passive particles*

For passive particles with $\Omega_{\rm f}\tau_{\rm f} = 0$ the most unstable wavenumber is

$$k_{\rm max}^2 H^2 = \sqrt{2\chi} - 1\,. \tag{2.20}$$

The wavenumber is real for $\chi \geqslant 0.5$. The maximum growth rate is

$$\gamma_{\rm max}/\Omega = (\sqrt{2\chi} - 1)^2 \frac{S_0}{c_{\rm s}^2 \rho_0}\,, \tag{2.21}$$

provided $\chi \geqslant 0.5$. For $\chi > 0.5$ there is growth even for zero friction time dust grains (which just trace the gas flow). In this case the increased gas density in the growing pressure bumps is enough to cause instability, from the passively advected dust grains. The growth rate with passive particles is also shown in Figure 1.

3. Outlook

To identify this new viscous instability in a numerical simulation we solve the resistive MHD equations in the standard shearing box approximation using the Pencil Code. We consider a box size of $L_x = 10.56H$, $L_y = 2.64H$, $L_z = 1.32H$ and a grid resolution of $256 \times 64 \times 32$. First we let the simulation run 20 orbits with only the constant hyper-resistivity needed to dissipate energy released by the turbulent stresses. After 20 orbits we turn on the density-dependent resistivity where regions of higher (lower) density have

https://doi.org/10.1017/S1743921311006569 Published online by Cambridge University Press

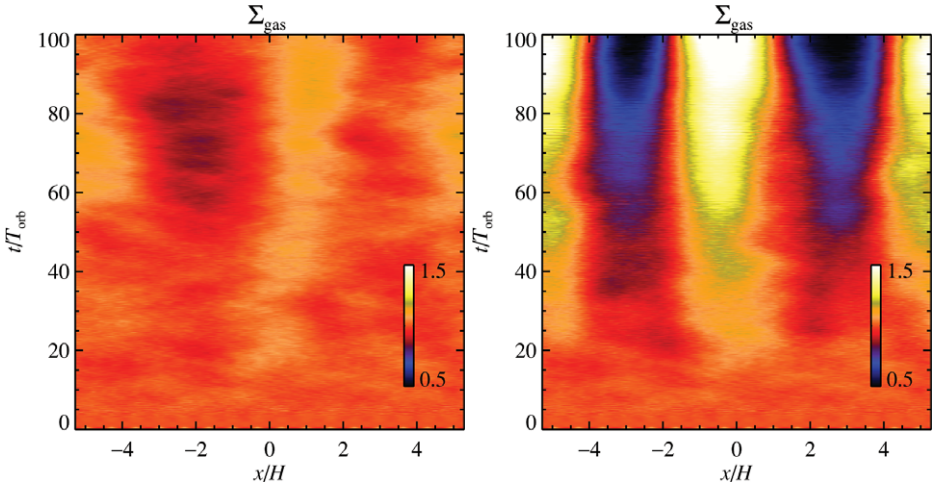

Figure 2. The evolution of the gas column density, averaged over the azimuthal direction, as a function of time. The left plot shows the results with constant hyperresistivity. Weak 5–10% level pressure bumps form on the largest scales of the turbulent flow (Johansen *et al.* 2009). Including dust-dependent resistivity, the right-hand plot shows the evolution of high-pressure regions with weak turbulence and low-pressure regions with high turbulence. This situation arises from the viscous instability driven by the dust-dependent resistivity of the gas.

higher (lower) resistivity. Figure 2 shows a space-time plot of the density. The emergence of a high-amplitude pressure bump is clear in the case of space-dependent resistivity.

The presence of pressure bumps in protoplanetary discs can have a positive effect on planet formation because the radial drift of particles is stopped in pressure bumps (particles seek the point of highest pressure, see e.g. Kato *et al.* 2009 and Johansen *et al.* 2009). Our new linear viscous instability can lead to the emergence of strong pressure bumps at the outer edge of the dead zone in protoplanetary discs. This makes the outer edge of the dead zone a prime site for planetesimal formation and thus for the rapid formation of the cores of gas giants. A paper in preparation details the non-linear evolution of the viscous instability (Kato *et al.* in preparation).

AJ and MK are grateful to Center for Planetary Sciences in Kobe for an extended visit that inspired this collaborative project. This work is supported in part by the Center for Planetary Science running under the auspices of the MEXT Global COE program entitled “Foundation of International Center for Planetary Science”.

References

Blaes, O. M. & Balbus, S. A., 1994, *The Astrophysical Journal*, 421, 163

Johansen, A., Youdin, A., & Klahr, H., 2009, *The Astrophysical Journal*, 697, 1269

Kato, M. T., Nakamura, K., Tandokoro, R., Fujimoto, M., & Ida, S. 2009, *The Astrophysical Journal*, 691, 1697

Okuzumi, S., 2009, *The Astrophysical Journal*, 698, 1122

Pessah, M. E., 2010, *The Astrophysical Journal*, 716, 1012

Sano, T., Miyama, S. M., Umebayashi, T., & Nakano, T., 2000, *The Astrophysical Journal*, 543, 486

https://doi.org/10.1017/S1743921311006569 Published online by Cambridge University Press